

## Weak light signal detection method for atomic gyroscope based on automatic zeroing of the bias

Wang Jing<sup>1,2</sup>, Zhou Binquan<sup>1,2</sup>, Wu Wenfeng<sup>1,2</sup>, Chen Linlin<sup>1,2</sup>, Zhao Xinghua<sup>1,2</sup>,  
Liang Xiaoyang<sup>1,2</sup>, Liu Gang<sup>1,2</sup>

(1. National Key Laboratory of Inertial Technology, Beijing 100191, China;

2. School of Instrument Science and Opto-electronics Engineering, Beihang University, Beijing 100191, China)

**Abstract:** Nuclear Magnetic Resonance Atomic Gyroscope has attracted an extensive attention due to its high precision, compact size and less cost at home and abroad. Among numerous techniques for obtaining the detection target, the balanced polarimetry technique is a more general method which monitors the rotation of the polarization plane of the probe beam. Due to miniaturization installation, the size effect is obvious. So there is an inevitable azimuth deviation between optical elements that leads to a bias of the weak optical signal, which extremely restricts the extraction and amplification. For the purpose of improving the detection performance, the differential detection principle of the laser polarization was analysed and a circuit method was proposed which could automatic eliminate the photodiode current bias based on the proportional-integral (P-I) feedback loop. A low-noise and high-gain preamplifier for silicon photodiode was presented. Finally, combined with the NMRG prototype system, the simulation analyses and experimental results were given, which verified the validity of this method.

**Key words:** NMRG; weak signal amplify; automatic zeroing of the bias; differential detection

**CLC number:** TN722.7    **Document code:** A    **DOI:** 10.3788/IRLA201847.0817004

## 基于自动消偏的原子陀螺微弱光信号检测方法

王 婧<sup>1,2</sup>, 周斌权<sup>1,2</sup>, 吴文峰<sup>1,2</sup>, 陈琳琳<sup>1,2</sup>, 赵兴华<sup>1,2</sup>, 梁晓阳<sup>1,2</sup>, 刘 刚<sup>1,2</sup>

(1. 惯性技术国家级重点实验室, 北京 100191;

2. 北京航空航天大学 仪器科学与光电工程学院, 北京 100191)

**摘 要:** 核磁共振原子陀螺凭借其高精度、小体积、低成本的特点在国内外受到广泛关注。在获取检测目标的诸多方法中,较为常用的方法是监测探测光极化面旋转角的平衡偏振法。由于小型化带来的尺寸效应明显,光学元件间存在不可避免的方位误差,导致微弱光信号产生偏置,制约了该信号的提取与放大。为提高检测性能,分析了激光偏振态的差分检测原理,提出了一种基于比例积分(P-I)反馈回路的自动消偏方法,设计了基于硅光二级管的低噪声、高增益前置放大电路。最后,结合核磁共振陀螺样机系统,给出了该方法的仿真分析和实验结果,验证了该方法的有效性。

**关键词:** 核磁共振陀螺; 微弱信号放大; 自动消偏; 差分检测

收稿日期:2018-03-05; 修订日期:2018-04-03

基金项目:国家自然科学基金(61627806,61227902)

作者简介:王婧(1993-),女,博士生,主要从事核磁共振陀螺方面的研究。Email:wangjing\_vicky@buaa.edu.cn

通讯作者:周斌权(1981-),男,讲师,博士,主要从事量子传感技术方面的研究。Email:bqzhou@buaa.edu.cn

## 0 Introduction

As a sensor for sensing angular velocity, gyro is a crucial component in inertial navigation<sup>[1]</sup>. Nuclear Magnetic Resonance Gyroscope (NMRG) is a new type of inertial device, which belongs to atomic gyroscopes<sup>[2]</sup>. With the development of MEMS<sup>[3]</sup> and integration technology, atomic devices can achieve a high level of integration. Nowadays, NMRG with advantages of high precision, compact size and less cost is becoming a promising alternative<sup>[4]</sup>. In 2016, Walker et al. proposed a brief overview of the NMRG built by Northrop Grumman Corporation, with ARW 0.005 (°)/h<sup>1/2</sup>, bias drift 0.02 (°)/h in a hermetic physics package of 10 cm<sup>3</sup><sup>[5]</sup>, which indicates the potential value of NMRG.

The main development trend of NMRG is miniaturization with a high accuracy. The rotation frequency is obtained by detecting the shift in Larmor frequency of nucleus in an applied magnetic field<sup>[6]</sup>. There is a probe beam propagating through a vapor cell to acquire this shift, and this weak optical signal is converted into electrical signal for subsequent circuit processing. While, there is an inevitable azimuth deviation between small optical elements that

leads to a bias of this signal, and the extraction and amplification performance is seriously affected. Only a tiny deviation between the incident light and PBS will result in a large bias. The AC amplitude to the bias ratio can even reach 1:100. Most of the existing preamplifier circuits cannot automatically eliminate this bias<sup>[7]</sup>. There is no relevant research aimed at solving this problem. Therefore, it is critical to find a suitable detection method.

In this paper, three main methods are reviewed, especially the balanced polarimetry technique. Analyses are conducted on the light route structure of the probe beam. Then, the adverse effects and the circuit design requirements are presented. Finally, a weak optical signal detection based on automatic zeroing the bias is proposed. Compared with direct output signal, using the proposed method, a low-noise and high-gain preamplifier with bias rejector, can effectively achieve remarkable performance.

## 1 Detection principle & demand

Figure 1 shows the basic measurement scheme for the dual isotope closed loop NMR gyro in which  $\omega_1$  and  $\omega_2$  imply the Lamor frequencies of 129 Xe and 131 Xe. Rb are spin-polarized by pump laser and

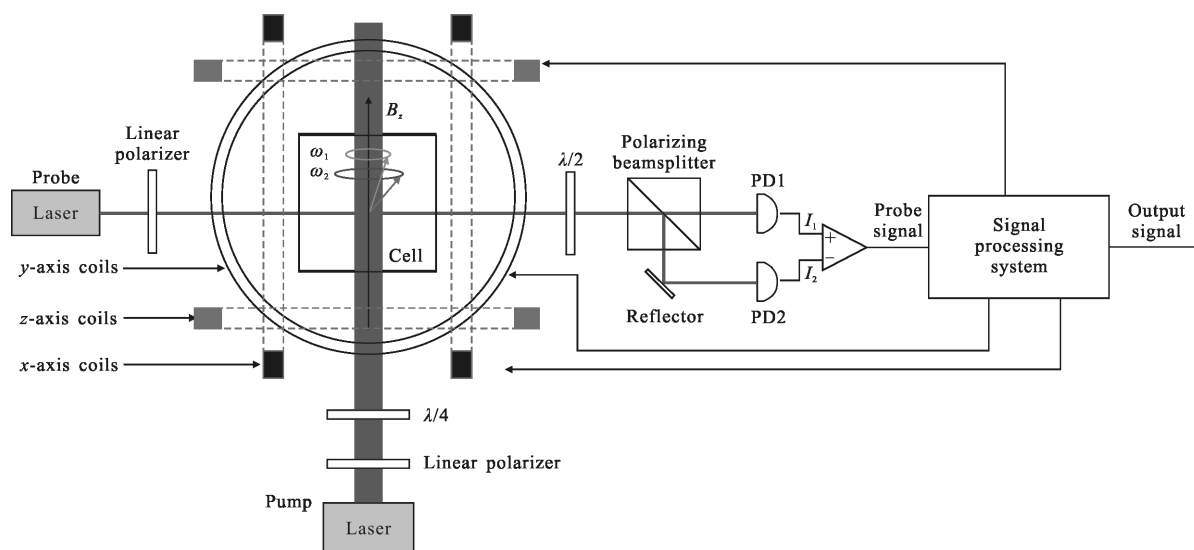


Fig.1 Basic measurement scheme for the dual isotope closed loop NMRG

transfer its angular momentum to Xe via collisions<sup>[8]</sup>. This precessing nuclear magnetization is detected by a sensitive atomic magnetometer, which is integrated into NMRG cell by alkali atoms<sup>[9]</sup>. There are numerous techniques to obtain this spin precession signal. The rotation of the polarization plane of the probe beam is proportional to the spin precession magnetic moment. Generally, an off-resonant, linearly polarized probe beam is used to reach this detected target<sup>[10]</sup>.

The commonly used methods for optical rotation measurements are Faraday modulation, photoelastic modulation, differential polarization<sup>[11]</sup>. The first two methods involve modulation of the light intensity, with good results for 1/f and low-frequency noise isolation. Thanks to the simple structure of differential polarization detection, it is easy to be integrated and miniaturized. However, the sensitivity of the third approach is not as good as the first two methods at low frequency, but it is more suitable for high-frequency occasion or devices with other modulation methods, such as NMRG<sup>[12]</sup>. Taking into account practicability and miniaturization, the third method has been chosen. For convenience, the basic structure of the differential polarization is taken out from Fig.1, as shown in Fig.2.

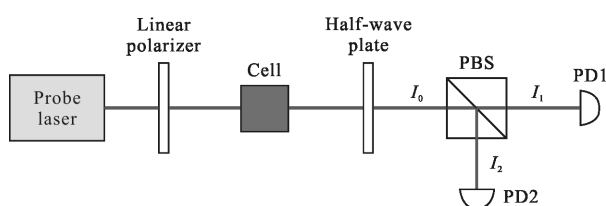


Fig.2 Light route structure of differential polarization detection

Before the cell, the probe beam is firstly adjusted to linearly polarized light. Then the probe beam incidents into the cell, and its polarization direction is altered by a half-wave plate. At last, the beam is split into two beams by PBS with individual intensities, hence the detected light intensities are:

$$I_1 = I_0 \cos^2(\theta - a), \quad I_2 = I_0 \sin^2(\theta - a) \quad (1)$$

where  $\theta$  is the rotation of the polarization plane of the probe beam which we expect to measure,  $a$  is the

incident light's initial polarization direction relative to PBS, as we called azimuth.  $I_0$  is the initial light intensity,  $I_1$  and  $I_2$  is the detected light intensities, such that  $I_0 = I_1 + I_2$ .

For  $\theta = 1$ , we can get a solution as:

$$\frac{I_1 - I_2}{2(I_1 + I_2)} = [\cos^2(\theta - a) - \sin^2(\theta - a)] I_0 / (2I_0) = \cos[2(\theta - a)] / 2 = \sin\left(2\theta - 2a + \frac{\pi}{2}\right) / 2 \approx \theta - a + \frac{\pi}{4} \quad (2)$$

When  $a = \frac{\pi}{4}$ ,  $\theta$  can be measured as:

$$\theta \approx \frac{I_1 - I_2}{2I_0} \quad (3)$$

It causes a problem that  $a = \frac{\pi}{4}$  cannot precisely get in an extremely small package. So, when there exists an azimuth error making  $a \neq \frac{\pi}{4}$ , a DC bias will be introduced into the optical signal.

As the intensity of the probe beam is modulated at Larmor frequency of <sup>87</sup>Rb which can be expressed in an applied magnetic field  $B_0$  as:

$$\omega_c = \gamma_{Rb} B_0 \quad (4)$$

where  $\gamma_{Rb} = 2\pi \times 6998 \text{ Hz}/\mu\text{T}$ , it is gyromagnetic ratio of <sup>87</sup>Rb, and  $B_0$  is about  $10 \mu\text{T}$ .

Based on the analysis above, the circuit design requirements of the detection are as follows:

- (1) The working frequency range is from 40 kHz to 200 kHz.
- (2) The DC offset is removed and a high gain amplification only for AC part.
- (3) The electronic noise should be avoided as much as possible.

## 2 Circuit design

This circuit selects silicon photodiode as the photodetector. It produces a small electric current proportional to the illumination when light falls on it<sup>[13]</sup> with the characteristics of high sensitivity, high reliability, fast response, and has been widely used.

This detection circuit consists of two parts, as shown in Fig.3. The first part is a trans-impedance amplifier, which contains a proportional-integrative (P-I) feedback loop to eliminate the bias. The AC

part of the photocurrent is converted into voltage. The second part is an inverting amplifier circuit, which can adjust the gain of the amplification.

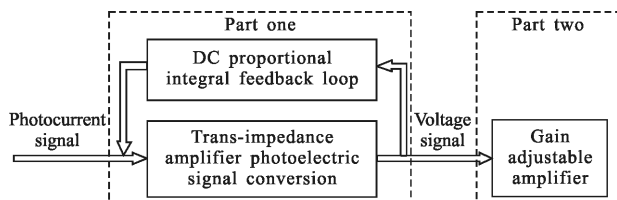


Fig.3 Block diagram of design structure

Figure 4 demonstrates this circuit structure in detail. It is made up of a few resistors, capacitances, unity-gain stable operational amplifiers (OP1, OP3), a high-gain differential amplifier (OP2). This part partially quotes the structure from reference [14]. The bias of the photocurrent is fed back to the starting point via this P-I loop. C<sub>3</sub> and R<sub>6</sub> serve as a high frequency filter, which can isolate the residual bias. Vo3 is the final output.

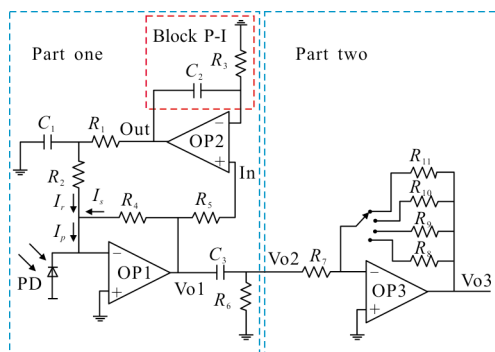


Fig.4 Principle diagram of the circuit

Using the concept of virtual short circuit and virtual open circuit, the output voltage of OP2 can be estimated as Eq.(5), where Vo1=in,

$$\text{out} = \text{in} + \int \frac{\text{in}}{R_3 C_2} \quad (5)$$

The circuit transfer function of the Vo1 and I<sub>p</sub> is obtained with an assumption that:

$$\frac{R_1 R_2}{R_1 + R_2} C_1 = R_3 C_2 \quad (6)$$

$$\frac{Vo1}{I_p} = \frac{R_4}{1 + \frac{R_4}{R_1 R_2 C_1 j \omega}} \quad (7)$$

where ω is the angular frequency, j is the imaginary unit. At high frequency ω ·  $\frac{R_4}{R_1 R_2 C_1}$ :

$$\left( \frac{Vo1}{I_p} \right)_{AC} = R_4 \quad (8)$$

Otherwise, the gain of the DC component is:

$$\left( \frac{Vo1}{I_p} \right)_{DC} = 0 \quad (9)$$

Relying on the structure of this circuit, we get a high-frequency gain on the AC part, and the gain vanishes on the DC part. The current signal of the photodiode has been amplified and converted into voltage signal through this two grades.

### 3 Simulation and experiment

We tested a design prototype with: R<sub>1</sub>=500 Ω, R<sub>2</sub>=10 kΩ, C<sub>1</sub>=10 μF, C<sub>3</sub>=10 μF, R<sub>6</sub>=1 MΩ, The circuit primary AC amplification is 10<sup>5</sup> V/A, the second is set to 10 V/A.

Figure 5 shows the simulation result of the output noise. The maximum output noise is about 3.6 μV, and the circuit output noise is far less than 1 μV in the working frequency range of 40:200 kHz. This noise is introduced by the circuit structure and device noises, which has a great influence on the circuit accuracy. It can be seen that this design produces little output noise which can meet our circuit requirement of low noise.

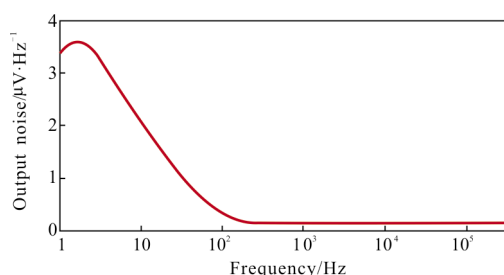


Fig.5 Output noise of the circuit

In order to illustrate the validity of this design, a sinusoidal current with DC bias is simulated using TINA, the simulation results are shown in Fig.6. This simulation current is a 100 kHz sinusoidal signal with amplitude 1 μA and bias 1 mA. The ratio of AC amplitude

and bias is  $\frac{1 \mu\text{A}}{1 \text{mA}} = 1:1\ 000$ , it is far ahead of our demand. The simulation results show the DC bias is completely isolated, and the AC part gets accurate and high gain amplification.

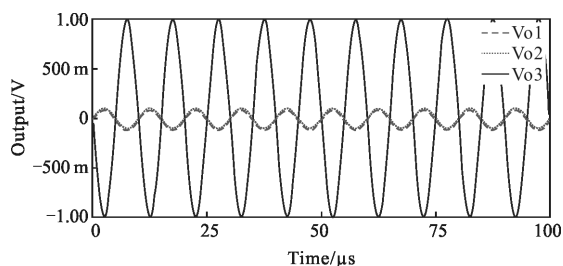


Fig.6 Simulation result of the sinusoidal signal with bias of 1 mA, frequency of 100 kHz, AC amplitude of 1 μA

The simulation results indicated the validity and the good low noise performance of the proposed circuit model. It illustrates this design is correct and effective. Based on the above analyses, finally a realized circuit prototype was made and tested. Figure 7 shows the realized circuit prototype.

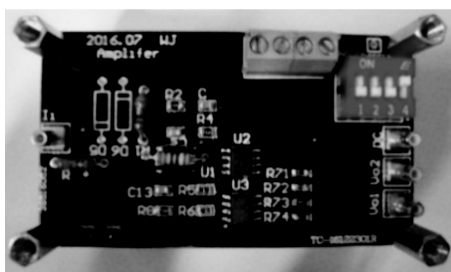


Fig.7 Realized circuit prototype

We firstly generated a modulation signal with a DC bias using Signal Generator, and then we put it as the input of our circuit and tested the output. The comparison was made between the output and the original signal, as shown in Fig.8. It can be clearly drawn from the curve in the figure that the amplification is accurate and the DC bias is completely eliminated. It has proven that it does have a good effect on eliminating DC-bias of the signal.

Finally, we tested it in our actual NMRG prototype. Because azimuth deviation leads to a bias in detection signal, to illustrate the benefit of our design, we initiatively adjust the plane direction of half-wave

plate to make an angle error between the incident light and PBS. The practical application results are shown in Fig.9. We can see from the experimental results that the design has achieved our goal.

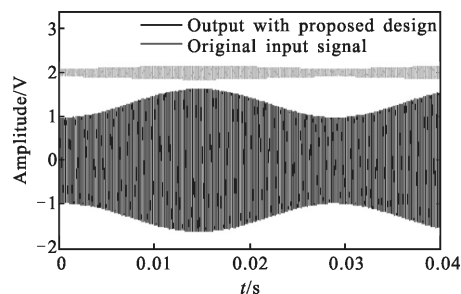
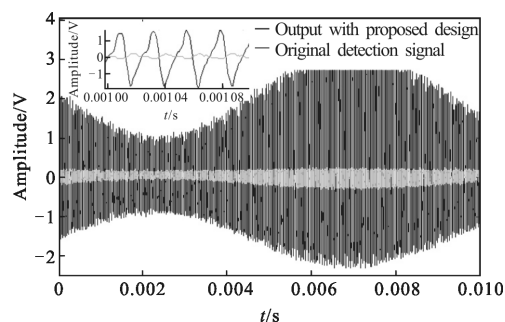
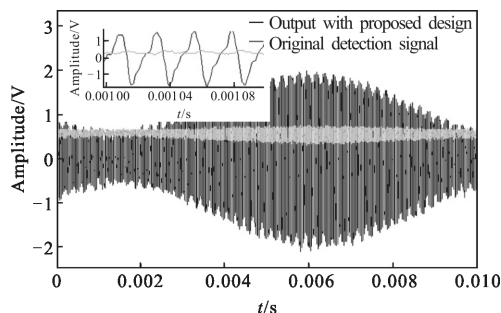


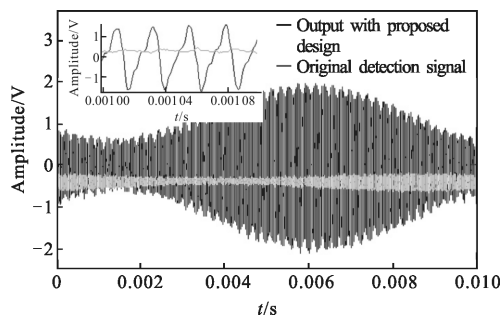
Fig.8. Comparison of the actual test result using this design and the original signal



(a) Azimuth error is zero, optical elements are in precise alignment



(b) Azimuth error is +0.05° and there exists a positive bias



(c) Azimuth error is -0.05° and there exists a negative bias

Fig.9 Contrast curve of the output signal of this design in different practical conditions

## 4 Conclusion

The detection principle and the adverse effects caused by azimuth error were investigated. Analyses were conducted on detection demands of the weak optical signal. At last, a weak optical signal detection method which had the function of zeroing the bias was proposed. The simulation and practice results verify the validity of this method. This circuit can also be used in other devices which need to suppress DC component and amplify current into voltage signal, such as vector atomic magnetometer.

### References:

- [1] Wang J P, Tian W F, Jin Z H. Study on integrated micro inertial navigation system/GPS for land vehicles [J]. *Intelligent Transportation Systems*, 2003, 2: 1650-1653.
- [2] Meyer D, Larsen M. Nuclear magnetic resonance gyro for inertial navigation [J]. *Gyroscopy and Navigation*, 2014, 5 (2): 75-82.
- [3] Schwindt P D, Lindseth B J, Shah V, et al. Chip-scale atomic magnetometer [J]. *Mine Warfare & Ship Self-Defence*, 2004, 85(26): 6409-6411.
- [4] Wang Wei. Development of new inertial technology and its application in aerospace field [J]. *Infrared and Laser Engineering*, 2016, 45(3): 0301003. (in Chinese)
- [5] Walker T G, Larsen M S. Spin-exchange-pumped NMR gyros[J]. *Advances in Atomic Molecular & Optical Physics*, 2016, 65: 373-401.
- [6] Donley E A. Nuclear magnetic resonance gyroscopes [J]. *Sensors IEEE*, 2010, 143(2): 17-22.
- [7] Wang Wai, Wu Wei, Feng Qi, et al. Design of a fully differential CMOS transimpedance preamplifier for 10 Gb/s optical receiver [J]. *Infrared and Laser Engineering*, 2015, 44(5): 1587-1592. (in Chinese)
- [8] Happer W, Miron E, Schaefer S, et al. Polarization of the nuclear spins of noble-gas atoms by spin exchange with optically pumped alkali-metal atoms [J]. *Physical Review A*, 1984, 29(6): 3092-3110.
- [9] Savukov I M, Romalis M V. NMR detection with an atomic magnetometer [J]. *Physical Review Letters*, 2004, 94 (12): 123001.
- [10] Chen L, Lei G, Wu W, et al. The optimal frequency and power of a probe beam for atomic sensor[C]//*Applied Optics and Photonics China*, 2015, 9671: 96711P.
- [11] Seltzer S J. Developments in alkali-metal atomic magnetometry[D]. Princeton: Princeton University, 2008.
- [12] Wan S. Study on experiment of error analysis and suppression methods for SERF atomic spin gyroscope [D]. Beijing: Beihang University, 2014. (in Chinese)
- [13] Peterson J D. Silicon photodiode: US, US2994054[P]. 1961-07-25.
- [14] Pullia A, Zocca F. Low-noise current preamplifier for photodiodes with DC-current rejector and precise intensity meter suited for optical light spectroscopy [C]//*Nuclear Science Symposium Conference Record*, 2010: 1343-1345.